Remote Sensing in Ecology and Conservation
Open Access
ZSL LET'S WORK FOR WILDLIFE

ORIGINAL RESEARCH

Detecting northern peatland vegetation patterns at ultra-high spatial resolution

Aleksi Räsänen[1], Mika Aurela[2], Sari Juutinen[1], Timo Kumpula[3], Annalea Lohila[2], Timo Penttilä[4] & Tarmo Virtanen[1]

[1]Ecosystems and Environment Research Programme, Faculty of Biological and Environmental Sciences, Helsinki Institute of Sustainability Science (HELSUS), University of Helsinki, Helsinki, Finland
[2]Finnish Meteorological Institute, Helsinki, Finland
[3]Department of Geographical and Historical Studies, Faculty of Social Sciences and Business Studies, University of Eastern Finland, Joensuu, Finland
[4]Natural Resources Institute Finland, Helsinki, Finland

Keywords
Drone, floristic analysis, lidar, northern boreal, unmanned aerial system (UAS), very-high spatial resolution

Correspondence
Aleksi Räsänen, Ecosystems and Environment Research Programme, Faculty of Biological and Environmental Sciences, and Helsinki Institute of Sustainability Science (HELSUS), University of Helsinki, Helsinki, Finland. Tel: +358504489001; E-mail: aleksi.rasanen@helsinki.fi

Editor: Ned Horning
Associate Editor: Jian Zhang

Received: 6 September 2019; Revised: 1 November 2019; Accepted: 21 November 2019

doi: 10.1002/rse2.140

Abstract

Within northern peatlands, landscape elements such as vegetation and topography are spatially heterogenic from ultra-high (centimeter level) to coarse scale. In addition to within-site spatial heterogeneity, there is evident between-site heterogeneity, but there is a lack of studies assessing whether different combinations of remotely sensed features and mapping approaches are needed in different types of landscapes. We evaluated the value of different mapping methods and remote sensing datasets and analyzed the kinds of differences present in vegetation patterns and their mappability between three northern boreal peatland landscapes in northern Finland. We utilized field-inventoried vegetation plots together with spectral, textural, topography and vegetation height remote sensing data from 0.02- to 3-m pixel size. Remote sensing data included true-color unmanned aerial vehicle images, aerial images with four spectral bands, aerial lidar data and multiple PlanetScope satellite images. We used random forest regressions for tracking plant functional type (PFT) coverage, non-metric multidimensional scaling ordination axes and fuzzy k-medoid plant community clusters. PFT regressions had variable performance for different study sites (R^2 −0.03 to 0.69). Spatial patterns of some spectrally or structurally distinctive PFTs could be predicted relatively well. The first ordination axis represented wetness gradient and was well predicted using remotely sensed data (R^2 0.64 to 0.82), but the other three axes had a less straightforward explanation and lower mapping performance (R^2 −0.09 to 0.53). Plant community clusters were predicted most accurately in the sites with clear string-flark topography but less accurately in the flatter site (R^2 0.16–0.82). The most important remote sensing features differed between dependent variables and study sites: different topographic, spectral and textural features; and coarse-scale and fine-scale datasets were the most important in different tasks. We suggest that multiple different mapping approaches should be tested and several remote sensing datasets used when maps of vegetation are produced.

Introduction

Northern peatlands store approximately 500 Gt of carbon, which is a substantial amount of the global terrestrial carbon stock (Loisel et al. 2017). Northern peatlands are also important in terms of biodiversity (Fraixedas et al. 2017; Saarimaa et al. 2019), water storage and hydrology (Waddington et al. 2015) and carbon exchange (Aurela et al. 1998, 2009; Loisel et al. 2017). Within peatlands, many biogeochemical cycles, such as flows of carbon, water and nutrients, are linked to vegetation (Loisel et al. 2017; Lees et al. 2018; McPartland et al. 2019). For

instance, the amount of green vegetation, often measured as leaf-area index or phytomass, is linked to carbon uptake capacity and release through mineralization within a specific landscape (Schneider et al. 2012; Peichl et al. 2015; Laine et al. 2019). As different plant species and communities have divergent habitat requirements, the vegetation structure at a given location indicates the moisture and trophic status; vegetation may thus be used as a proxy for biogeochemical fluxes (Davidson et al. 2017; Bradley-Cook and Virginia 2018). Mapping of vegetation is also important in showing the spatial patterns of species distribution and biodiversity (Saarimaa et al. 2019).

Remotely sensed data enables mapping of vegetation patterns. It has been discussed that continuous maps of vegetation properties, such as ordination axes, fuzzy plant community clusters or plant functional types (PFTs), capture the vegetation patterns more realistically and ecologically more meaningfully than categorical land-cover maps (Ustin and Gamon 2010; Rocchini 2014; Harris et al. 2015; Rapinel et al. 2018; Räsänen et al. 2019b). Ordination methods are used to quantify floristic (dis)similarity between vegetation plots; thus, maps of ordination axis scores represent floristic gradients (Feilhauer et al. 2011; Harris et al. 2015). In turn, when mapping floristically defined plant communities, it has been argued that fuzzy clustering approaches should be preferred as plant communities seldom have clear boundaries and may overlap spatially (Rocchini 2014; Rapinel et al. 2018; Räsänen et al. 2019b). PFTs are a way of grouping plant species based on their growth forms, life strategies and responses to environmental conditions (Chapin et al. 1996; Duckworth et al. 2000; Ustin and Gamon 2010; Hartley et al. 2017). Maps of PFTs are especially valuable in biogeochemical modeling purposes and in mapping ecosystem functioning, such as ecosystem photosynthesis and net carbon exchange (Ustin and Gamon 2010; Schmidtlein et al. 2012; Kattenborn et al. 2019). There are different types of PFT classifications (Duckworth et al. 2000; Ustin and Gamon 2010). For instance, grouping into evergreen and deciduous shrubs, forbs, graminoids and mosses is a widely used approach when mapping biomass and leaf-area index patterns (Juutinen et al. 2017; Berner et al. 2018; Räsänen et al. 2019a) or in Earth system models (Poulter et al. 2015; Dallmeyer et al. 2019).

It has been shown that multiple different remote sensing features and data types should be included when mapping vegetation patterns because different datasets complement each other by providing different types of information (Chen et al. 2017; Räsänen and Virtanen 2019). The different types of information include, for instance, reflectance of vegetation and other land cover which can be obtained from passive imagery data from multiple different platforms, including Unmanned Aircraft Vehicles (UAV), aerial and satellite (Middleton et al. 2012; Harris et al. 2015; Kalacska et al. 2015; Palace et al. 2018). The reflectance patterns vary in space and time, and it has been shown that inclusion of spatial variability (i.e. texture) (Hall-Beyer 2017; Chen et al. 2018; Mishra et al. 2018) and temporal variability indicating phenology (Chen et al. 2017; Halabisky et al. 2018) increases mapping performance when detecting vegetation and land-cover patterns. Furthermore, it has been shown that information about topography and vegetation structure should be included in mapping tasks. Topography and vegetation structure can be captured with photogrammetry or active remote sensing methods, including structure-from-motion photogrammetry and lidar (Mercer and Westbrook 2016; Franklin and Ahmed 2017; Shadaydeh et al. 2017; Sankey et al. 2018; Prošek and Šímová 2019; Räsänen and Virtanen 2019; Scholefield et al. 2019). Finally, there are scalar differences within land cover and vegetation structure and reflectance, ranging from leaf via canopy to landscape (Kalacska et al. 2015; Rautiainen et al. 2018; Riihimäki et al. 2019), suggesting that data from multiple different spatial resolutions should be included in mapping endeavors (Räsänen and Virtanen 2019; Riihimäki et al. 2019).

Within northern peatlands, landscape elements such as vegetation, topography, moisture and trophic status vary in multiple spatial scales. Some of the spatial differences are evident in centimeter-level spatial resolution (i.e. ultra-high spatial resolution) (Lehmann et al. 2016; Mercer and Westbrook 2016; Lees et al. 2018; Palace et al. 2018; Räsänen et al. 2019b). Other differences, such as broad-scale moisture gradients, have a coarser spatial scale (Middleton et al. 2012; Harris et al. 2015; Saarimaa et al. 2019). Within a single peatland, both fine-scale and coarse-scale spatial heterogeneity can be found (Harris et al. 2015), and different peatland landscapes have divergent spatial heterogeneity patterns.

We argue that the differences between different northern peatlands indicate a need for comparisons between sites. Furthermore, to the best of our knowledge, there is a lack of studies assessing whether different combinations of remotely sensed features and different mapping approaches should be used when different types of peatland landscapes are studied. Therefore, our aim was to compare sites, remote sensing datasets and mapping approaches in detecting peatland vegetation patterns. We mapped PFT %-coverage, vegetation ordination axes and fuzzy plant community clusters in three northern boreal peatland landscapes in northern Finland with the assistance of field inventoried vegetation plots and remotely sensed data in 0.02-m to 3-m pixel size. We asked three research questions. Firstly, how well can peatland

vegetation patterns be delineated with multisource and multiresolution remotely sensed data? Secondly, what are the optimal mapping methods and remote sensing datasets? Thirdly, what kind of differences are there in the mappability of vegetation patterns between different northern peatland study sites?

Materials and Methods

Study sites

To estimate differences in the mappability of vegetation patterns between different northern peatland ecosystems, we analyzed three contrasting treeless fens in northern Finland (Fig. 1). The sites are located in a northern boreal vegetation zone 100–200 km apart from each other but have differing microtopographic variability (i.e. landscape heterogeneity) offering thus an attractive comparison triad. Continuous eddy covariance measurements of CO_2 and CH_4 exchange have been running at all three sites for several years. The vegetation patterns have also been studied extensively at all sites (Aurela et al. 1998, 2004, 2009; Maanavilja et al. 2011; Lohila et al. 2015; Dinsmore et al. 2017; Räsänen and Virtanen 2019; Räsänen et al. 2019b). Nevertheless, the vegetation data have not been compared between the sites, and the utilization of remote sensing analyses of vegetation has been limited.

The northernmost site, Kaamanen, is characterized by a strong pattern of dry strings covered by evergreen shrubs and feather mosses and wet flarks with graminoid and wet brown moss vegetation and periodical water cover (Aurela et al. 1998, 2004; Maanavilja et al. 2011; Räsänen and Virtanen 2019; Räsänen et al. 2019b). The dry strings are up to 1 m high and 5 m wide and form a continuous network in a winding pattern. A stream running through the fen has riparian areas with tall sedge, deciduous shrub

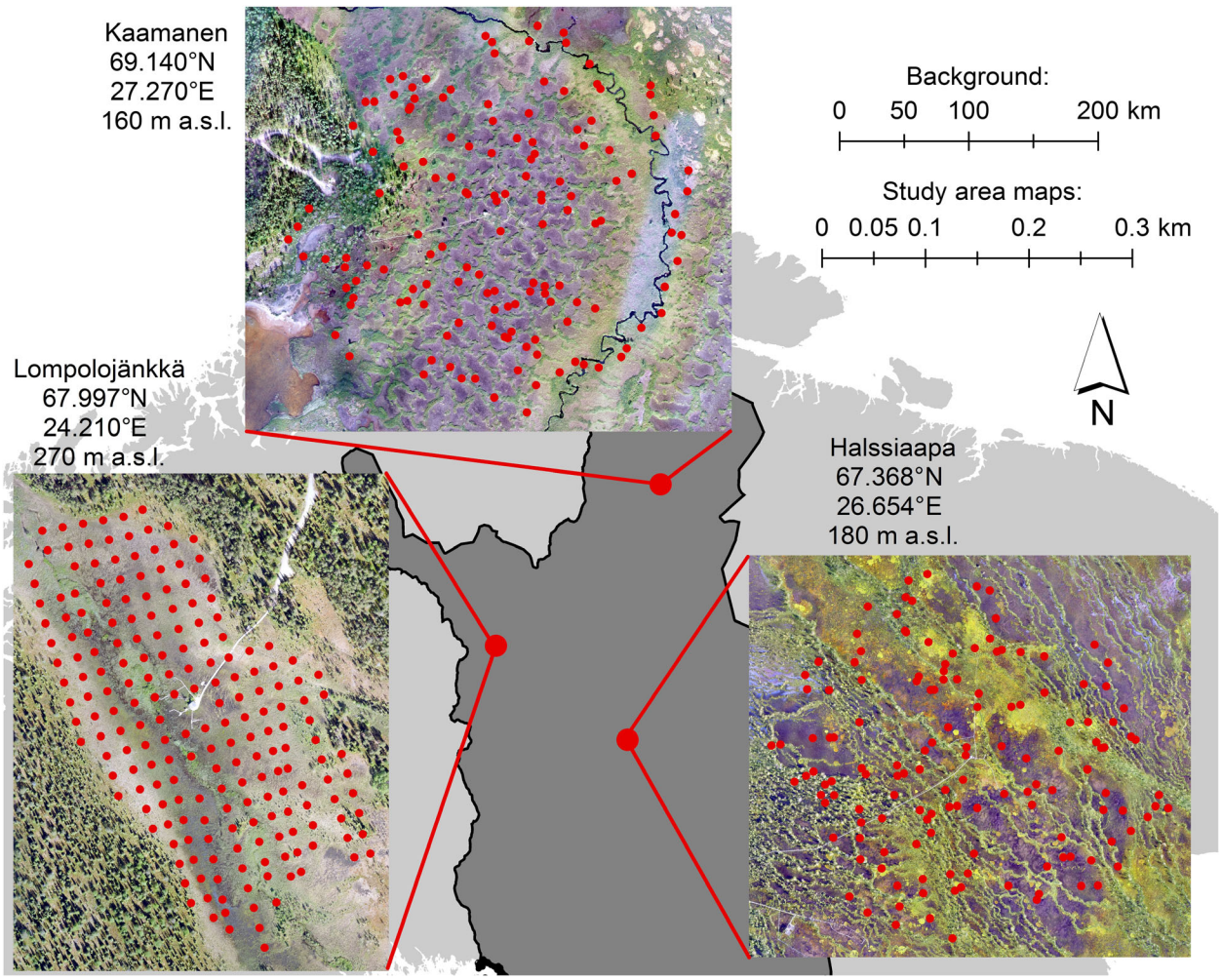

Figure 1. Location of study sites in northern Finland. Field inventory plots in each study site are drawn on a true-color unmanned aerial vehicle image. Images were taken on Aug 1, 2018 (Kaamanen), Jun 17, 2018 (Lompolojänkkä) and Jul 12, 2016 (Halssiaapa).

and forb vegetation; a pine bog zone is found at the edge of the fen. In previous studies, four to five different plant communities have been identified, representing string top, string margin, wet flark, graminoid flark and riparian fen communities (Maanavilja et al. 2011; Räsänen et al. 2019b).

Lompolojänkkä fen, located in Pallas, has a rather flat surface patterning and is characterized by mesotrophic vegetation (Aurela et al. 2009; Lohila et al. 2015). A small stream runs through the study site and its riparian areas are vegetated by approximately 60-cm-high *Salix* thickets. In the middle parts of the fen, affected by a continuous surface water flow, the vegetation patterns are dominated by *Sphagnum* and wet brown mosses, graminoids, low shrubs and some forbs. In the edges of the fen, oligotrophic *Sphagnum*-evergreen shrub vegetation can be found.

The southernmost site, Halssiaapa fen in Sodankylä (Dinsmore et al. 2017; Räsänen et al. 2019a), has evident fine-scale heterogeneity in wetness and trophic status patterns. However, the transitions between different vegetation and microforms are more gradual than in Kaamanen and the low strings dominated by *Sphagnum* and evergreen shrubs are only some decimeters above the wet flarks dominated by wet brown mosses and some graminoids. In between the flarks and strings, there are lawns with continuous *Sphagnum* cover and forbs. Trophic status varies from oligotrophic to eutrophic.

Field inventories

We sampled 141, 201 and 140 square plots with 50-cm side length in July 2018 in Kaamanen, Lompolojänkkä and Halssiaapa respectively (Fig. 1). We chose sampling protocols so that all relevant land cover and vegetation types within the study sites could be covered. In Kaamanen and Halssiaapa, we could use existing land-cover type mappings (Räsänen et al. 2019b; Mikola et al. unpublished data), and we used stratified random sampling with strata being different land-cover types. The plots were located a minimum of 3 m apart from each other and a maximum of 200 m apart from the flux tower. In Lompolojänkkä, we had no existing land-cover map and sampled the plots systematically with a 20-m distance from each other. The plots were geolocated with a Trimble R10 GPS device with ±5 cm accuracy. We identified vascular plant and moss species at species level and evaluated their %-coverage with visual interpretation.

Remote sensing datasets

Our aim was to include a versatile set of different remote sensing datasets in order to address research question 2 and to test what kind of datasets and features are the most important when mapping different vegetation properties in different study sites. We gathered remote sensing data about spectral, topography and vegetation height properties captured from UAV, aerial and satellite platforms with 0.02-m to 3-m spatial resolution (Table 1). We calculated the mean value of different layers within each field inventory plot. In total, we had 75 (Kaamanen), 87 (Lompolojänkkä) and 84 (Halssiaapa) remote sensing features (Table 1).

In all study sites, we used two true-color UAV images collected by the authors and field technicians (Table 1). In Kaamanen, the images were from July 2017 and August 2018; in Lompolojänkkä, from June and August 2018 and in Halssiaapa, from July 2016 and July 2018. The inclusion of two images provided information from a wetter and drier year (Kaamanen and Halssiaapa) and from early and late summer (Lompolojänkkä). In Kaamanen and Halssiaapa, the images were acquired with DJI phantom 4 pro and in Lompolojänkkä with an eBee Plus fixed-wing drone and Matrice 210 quadrocopter.

We processed the UAV data using structure-from-motion photogrammetry and produced centimeter-resolution image mosaics (pixel size 2–5 cm) and digital terrain models (DTM) (pixel size 8–13 cm) for each study site (Table 1). In Kaamanen, we georeferenced the 2018 UAV data with 15 ground control points and the 2017 data with 14 points. In Lompolojänkkä, the June image was georeferenced with real-time kinematic positioning, later verified with the assistance of 13 ground control points. The August image was co-registered with the June image using 17 control points. In Halssiaapa, the 2018 image was georeferenced with 15 ground control points, and the 2016 image was co-registered with the 2018 image using 20 control points. All ground control points were geolocated with a Trimble R10 GPS device with ± 5 cm accuracy.

From the UAV DTM, we calculated the following topographical features: elevation, slope in degree, topographic position index (TPI) (Guisan et al. 1999) with 2-m and 5-m neighborhood radius and topographic wetness index (TWI) (Böhner and Selige 2006) (Table 1). We also calculated the following eight gray-level co-occurrence matrix textural features (Haralick et al. 1973) for each spectral band of the July/August 2018 UAV images: energy (texture uniformity), entropy (texture randomness), correlation (pixel correlation with its neighborhood), inverse difference moment (texture homogeneity), inertia (intensity contrast between a pixel and its neighborhood), cluster shade, cluster prominence and Haralick correlation. These were calculated with eight quantization levels and a moving window technique with the neighborhood distance set to five.

Table 1. Remote sensing datasets and layers used

Dataset	Date	Producer	Spatial resolution	Number and list of layers
UAV image 1	Aug 1, 2018 (Kaamanen) Aug 20, 2018 (Lompolojänkkä) July 11, 2018 (Halssiaapa)	Authors	0.03 m (Kaamanen) 0.02 m (Lompolojänkkä) 0.02 m (Halssiaapa)	27: B, G, R, and 8 GLCM layers from all spectral bands
UAV image 2	Jul 1, 2017 (Kaamanen) Jun 17, 2018 (Lompolojänkkä) Jul 12, 2016 (Halssiaapa)	Authors	0.05 m (Kaamanen) 0.04 m (Lompolojänkkä) 0.02 m (Halssiaapa)	3: B, G, R
UAV digital elevation model	Aug 1, 2018 (Kaamanen) Aug 20, 2018 (Lompolojänkkä) July 11, 2018 (Halssiaapa)	Authors	0.13 m (Kaamanen) 0.08 m (Lompolojänkkä) 0.09 m (Halssiaapa)	5: Elevation, slope, TPIs (2 m and 5 m distance), TWI
Aerial image	Jun 26, 2016 (Kaamanen) Jul 1, 2018 (Lompolojänkkä) Aug 19, 2015 (Halssiaapa)	National Land Survey of Finland	0.5 m	4: B, G, R, NIR
Lidar data	Jul 12, 2016 (Kaamanen) Jul 13, 2018 (Lompolojänkkä) Aug 19, 2015 (Halssiaapa)	National Land Survey of Finland	0.5 points m^{-2} (point cloud) 2 m (layers)	9: Elevation, slope, TPIs (5 m, 10 m, 20 m, 50 m, 100 m distances), TWI, CHM
PlanetScope images	May 25, Jun 16, Jul 2, Jul 10, Jul 19, Jul 29, Aug 26, Sep 9, Sep 25, 2018 (Kaamanen) May 25, May 31, Jun 17, Jul 1, Jul 11, Jul 19, Jul 29, Aug 10, Aug 18, Aug 26, Sep 2, Sep 9, Sep 21, 2018 (Lompolojänkkä) May 16, Jun 2, Jun 17, Jul 3, Jul 10, Jul 19, Jul 27, Aug 8, Aug 26, Sep 9, Sep 18, Oct 4, 2018 (Halssiaapa)	Planet Labs Inc.	3 m	27 (Kaamanen) 39 (Lompolojänkkä) 36 (Halssiaapa) NDVI, NDWI, RGI from all images

Abbreviations: B, blue; CHM, canopy height model; G, green; GLCM, gray-level co-occurrence matrix; NDVI, normalized difference vegetation index; NDWI, normalized difference water index; NIR, near-infrared; R, red; RGI, red-green index; TPI, topographical position index; TWI, topographical wetness index; UAV, unmanned aerial vehicle.

To capture coarser-resolution topography and spectral patterns as well as vegetation height information, we utilized aerial orthophotos with four bands and 50-cm resolution, and lidar data from the National Land Survey of Finland (Table 1). From lidar data, we used 2-m resolution DTM preprocessed by the National Land Survey and calculated elevation, slope, TPI (Guisan et al. 1999) with 10-m, 20-m, 50-m and 100-m neighborhood radius and TWI (Böhner and Selige 2006) (Table 1). We also computed a digital surface model from the lidar point cloud using all returns and then subtracted DTM from the digital surface model to obtain a canopy height model (CHM) (Table 1).

To track the impact of phenology throughout the summer, we utilized the surface reflectance product of PlanetScope satellite images (Planet Team 2017) from images taken between mid-May and early October 2018 (Table 1). For each study site, we used all available cloud-free images if they were a minimum of 6 days apart from each other. We included 9, 13 and 12 images from Kaamanen, Lompolojänkkä and Halssiaapa respectively. We calculated the normalized difference vegetation index (NDVI) (Rouse et al. 1974), normalized difference water index (NDWI) (McFeeters 1996) and red-green index (RGI) (Coops et al. 2006) for each image (Table 1).

Statistical analyses

To test the mappability of different vegetation properties and address research questions 1 and 2, we mapped PFTs, non-metric multidimensional scaling (MDS) (Kruskal 1964a,b) ordination axes and fuzzy k-medoid (Krishnapuram et al. 2001) cluster membership values. With all of these methods, continuous maps of vegetation could be constructed. In all tasks, we conducted random forest regressions (Breiman 2001) and predicted the vegetation properties for field inventory plots with the calculated remote sensing features.

For estimating PFT abundance (%) using regression models, we calculated the %-coverage of the following groups for each field inventory plot: evergreen dwarf shrubs, deciduous dwarf shrubs, forbs, graminoids, wet brown mosses, feather mosses and *Sphagnum* mosses. In Lompolojänkkä, we also calculated the %-coverage of *Salix* spp. The amount of *Salix* spp. was very low in other study sites. In addition, we added up the overall %-

coverage of all shrubs, all vascular plants and all mosses. Similar PFT classification has been used previously, for example, in Hugelius et al. (2011) and Räsänen et al. (2019a), and it fits well with classifications presented in Chapin et al. (1996).

For ordination axis regressions, we derived the axes using non-metric MDS of a distance matrix of plot and species-specific %-coverages. We transformed data values with Wisconsin double standardization and square root transformation, calculated the distance matrix with Bray–Curtis distances (Bray and Curtis 1957) and tested 20 random starts. We tested a different number of axes by evaluating the amount of stress in scaling and used four axes, as after that there was only a marginal reduction in the amount of stress (<0.03).

We delineated fuzzy k-medoid clusters from the four ordination axes. In fuzzy k-medoids, representative objects (i.e. medoids) for each cluster are selected so that within-cluster fuzzy dissimilarity is minimized (Krishnapuram et al. 2001). Fuzzy k-medoid is less sensitive to outliers than fuzzy k-means algorithm and can thus be considered a robust method (Ferraro and Giordani 2015). We sought the optimal number of clusters using fuzzy silhouette, which has been shown to perform robustly when evaluating fuzzy cluster validity (Campello and Hruschka 2006). We predicted cluster membership values for each fuzzy cluster. In addition, we predicted crisp cluster for each plot (i.e. the majority cluster) and evaluated the indicator species for each crisp cluster using Dufrene–Legendre indicator value analysis (Dufrêne and Legendre 1997). We set the fuzziness parameter to 1.5, the number of clusters between 2 and 10 and the weighting coefficient for the fuzzy silhouette to 1.

In random forest regressions, we set the number of features tested at each split to one-third of the number of features in regression and the number of trees in each regression to 500. In all regressions, we reduced the number of features using a Boruta feature selection algorithm (Kursa and Rudnicki 2010). Boruta is a random forest wrapper algorithm in which those features are removed from subsequent runs whose importance is significantly lower than the maximum importance of randomly derived shadow features. We used the mean decrease in accuracy measure when evaluating feature importance and chose all non-rejected features after 999 random forest runs to the final random forest regressions. We also assessed the relative feature importance of non-rejected features by calculating the average mean decrease in accuracy value over the 999 runs.

We evaluated the regression performance using a random forest out-of-bag estimation of percentage of variance explained (pseudo $R^2 = 1 -$ (mean squared error)/variance(response)). In out-of-bag, two-thirds of the data in each tree are used for training and the remainder for model evaluation (Breiman 2001); out-of-bag error statistics have shown to be unbiased or even slightly conservative when compared to an independent test dataset (Clark et al. 2010). We assessed what amount of variation in the Bray–Curtis distance matrix is explained by the four ordination axes and fuzzy cluster membership values by using permutational multivariate analysis of variance (PERMANOVA) (Anderson 2001).

Analyses were conducted in R (R Core Team 2018) using the packages randomForest (Liaw and Wiener 2002), Boruta (Kursa and Rudnicki 2010), vegan (Oksanen et al. 2018) and fclust (Ferraro and Giordani 2015).

Results

Plant functional type regressions

PFT regressions had a variable performance for different study sites and PFTs (Table 2). In Kaamanen, R^2 was >0.6 for evergreen shrubs as well as shrubs and vascular plants in total and between 0.4 and 0.6 for deciduous shrubs, forbs and feather mosses. In Lompolojänkkä, R^2 was >0.5 for *Salix* spp. and >0.3 for *Sphagnum* and mosses in total. R^2 values were seemingly low for other PFTs. In Halssiaapa, R^2 was >0.5 for *Sphagnum*, wet brown mosses and vascular plants, and between 0.4 and 0.5 for deciduous shrubs, forbs and shrubs in total. The performance was poor in all study sites for graminoids.

Ordination analysis and plant community clusters

In total, 85 (Kaamanen), 94 (Lompolojänkkä) and 66 (Halssiaapa) plant species were identified. When the species distance matrix was simplified with the four MDS axes, the stress was 0.09 in Kaamanen, 0.16 in Lompolojänkkä and 0.13 in Halssiaapa. According to PERMANOVA, the four-first MDS axes explained 44% (Kaamanen), 37% (Halssiaapa) and 28% (Lompolojänkkä) of the variation in the species distance matrix.

The first MDS axis represented the wetness gradient in all study sites and could be reasonably well explained using remotely sensed data (R^2 0.82 in Kaamanen, 0.64 in Lompolojänkkä and 0.68 in Halssiaapa) (Table 2). In Kaamanen and Halssiaapa, species occurring in wet habitats had high scores on the first axis, whereas the opposite pattern was observed in Lompolojänkkä (Figs. 2–4). In Kaamanen and Lompolojänkkä, the second MDS axis was also reasonably well predicted (R^2 0.53 and 0.49 respectively), whereas in Halssiaapa, prediction capability was higher for the third axis (R^2 0.40) (Table 2). In Kaamanen, the second MDS axis represented surface water

Table 2. Percentage of variation (R^2) explained in random forest regressions for different plant functional types, multidimensional scaling (MDS) axes and clusters

Regression	Kaamanen (R^2)	Lompolojänkkä (R^2)	Halssiaapa (R^2)
Salix	–	0.55	–
Evergreen shrubs	0.62	0.01	0.23
Deciduous shrubs	0.41	0.11	0.46
Shrubs total	0.62	0.22	0.44
Forbs	0.49	0.14	0.41
Graminoids	0.26	−0.03	0.04
Vascular plants total	0.69	0.15	0.54
Sphagnum	0.16	0.32	0.63
Wet brown mosses	0.38	0.16	0.57
Feather mosses	0.44	0.04	0.03
Mosses total	0.15	0.36	0.14
MDS1	0.82	0.64	0.68
MDS2	0.53	0.49	0.22
MDS3	0.31	0.26	0.40
MDS4	0.15	0.21	−0.09
Cluster 1	0.45	0.16	0.59
Cluster 2	0.76	0.29	0.58
Cluster 3	0.43	0.44	–
Cluster 4	0.82	0.26	–
Cluster 5	–	0.58	–

impact, with species occurring in nearby streams having high values (Fig. 2). The second axis at Lompolojänkkä and Halssiaapa as well as the third and fourth axes at all sites had a less evident ecological interpretation (Figs. 3–4, and Figs. S1–S3).

The optimal number of clusters was four in Kaamanen (explaining 42% of the variation in the distance matrix based on PERMANOVA), five in Lompolojänkkä (explaining 21% of the variation) and two in Halssiaapa (explaining 22% of the variation).

In Kaamanen, the two clusters that represented the extreme ends of the wetness gradients could be predicted with high accuracy, with R^2 values being 0.76 for the dry string cluster 2 and 0.82 for the wet flark cluster 4 (Fig. 2, Table 2). R^2 values were <0.5 for the two other clusters that were partly overlapping and characterized by surface water impact and taller vegetation (graminoid-dominated cluster 1 and tall deciduous shrub cluster 3).

In Lompolojänkkä, clusters included one drier and four wetter clusters (Fig. 3). Of these, the dry and oligotrophic cluster 5 dominated by shrubs and sphagnum mosses could be predicted reasonably well (R^2 0.58). R^2 was also moderately high (0.44) for the cluster 3 found adjacent to the stream and dominated by tall *Salix* spp., *Comarum palustre* and *Carex aquatilis* vegetation. The three other clusters (i.e. graminoid dominated cluster 1, *Betula nana-Salix* cluster 2 and *Sphagnum*-low shrub cluster 4) had R^2 values < 0.3 (Table 2).

In Halssiaapa, clusters represented dry string (cluster 1) and wet flark (cluster 2) plant communities had reasonably high R^2 in the remote sensing-based regressions (0.59 and 0.58 respectively) (Table 2, Fig. 4). The drier cluster 1 had more indicator species and higher variation both on the first and second MDS axis (Fig. 4).

Feature importance

Topographic, spectral and textural features were among the most important predictors in regressions, and the most influential remote sensing features varied between sites and models (Fig. 5, Tables S2–S4). In different regressions, the number of non-rejected features ranged between 2 and 43. In Kaamanen, particularly, UAV-based topographic features and lidar features were among the most important ones (Fig. 5A). However, PS indices and aerial image and UAV bands were also on the top-40 list. Of these, the PS indices were among the most important in the MDS and cluster regressions, but not in the PFT regressions (Table S2). In addition, texture features were typically rejected in different Boruta runs. PS indices were among the most important features in Lompolojänkkä; some lidar and aerial image features were also highly important (Fig. 5B). In contrast, there were only a few important UAV-based features. However, in *Salix* and Cluster 3 regressions, which had relatively high R^2 (Table 2), many of the UAV texture features were influential (Table S3). In Halssiaapa, both spectral and topographic UAV features and aerial image bands were included in the top-ranked features (Fig. 5C). Some PS indices were also deemed important, but many of the PS indices and lidar features were usually rejected (Table S4).

Discussion

While vegetation patterns could be mapped to some extent in all study sites, the mapping performance was best in Kaamanen, followed by Lompolojänkkä and Halssiaapa (Table 2). PFT regression models had relatively good explanatory capacity in Kaamanen but seemingly low in Lompolojänkkä. However, in all study sites, spatial patterns of some spectrally or structurally distinctive PFTs could be predicted relatively well. These included *Sphagnum* in Halssiaapa and *Salix* spp. in Lompolojänkkä. In all study sites, the first ordination axis had meaningful ecological interpretation and was well predicted using remotely sensed data. However, the picture was less clear for other ordination axes (Figs. 2–4 and Figs. S1–S3). Clusters were predicted most accurately in Kaamanen and Halssiaapa with string-flark topography but less accurately in flatter Lompolojänkkä (Table 2). The prediction accuracy is linked both to the number of

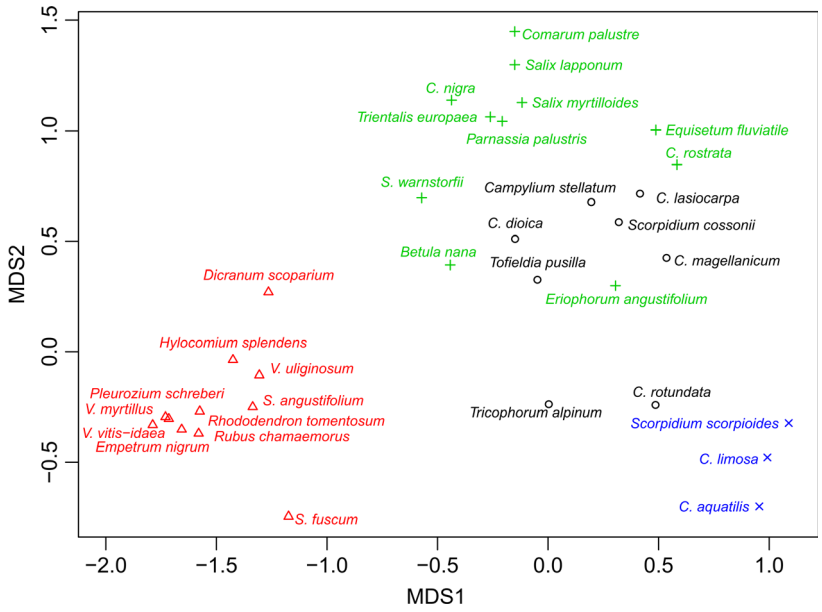

Figure 2. Non-metric multidimensional scaling (MDS) ordination axes and plant community clusters for Kaamanen study site. The statistically significant (P-value < 0.05) indicator species for different clusters drawn on an ordination plot where non-metric multidimensional scaling axis 1 is on x-axis and axis 2 on y-axis. Cluster 1 is shown with black, cluster 2 with red, cluster 3 with green and cluster 4 with blue. Species indicator values are given in Table S1. "C." refers to Carex, "S." to Sphagnum and "V." to Vaccinium.

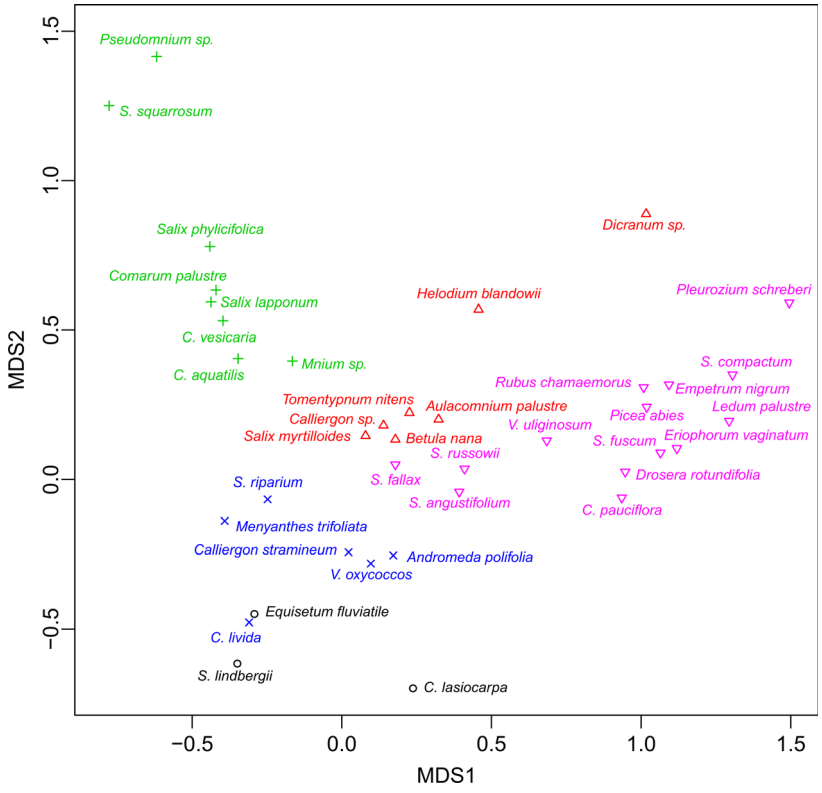

Figure 3. Non-metric multidimensional scaling (MDS) ordination axes and plant community clusters for Lompolojänkkä study site. The statistically significant (P-value < 0.05) indicator species for different clusters drawn on an ordination plot where non-metric multidimensional scaling axis 1 is on x-axis and axis 2 on y-axis. Cluster 1 is shown with black, cluster 2 with red, cluster 3 with green, cluster 4 with blue, and cluster 5 with pink. Species indicator values are given in Table S1. "C." refers to Carex, "S." to Sphagnum and "V." to Vaccinium.

clusters (two in Halssiaapa and five in Lompolojänkkä) and to the properties of each cluster (easily separable in Kaamanen). In all study sites, different types of remotely sensed features were needed in mapping tasks, suggesting that future mapping endeavors should include mixtures of datasets (Fig. 5).

The good mapping performance (Table 2) in Kaamanen was probably related to the distinctive patterns in vegetation and microtopography. Vegetation in such environments has also been easy to map in earlier studies (Lehmann et al. 2016; Palace et al. 2018). Microtopographical patterns were visible in ordination axes, plant

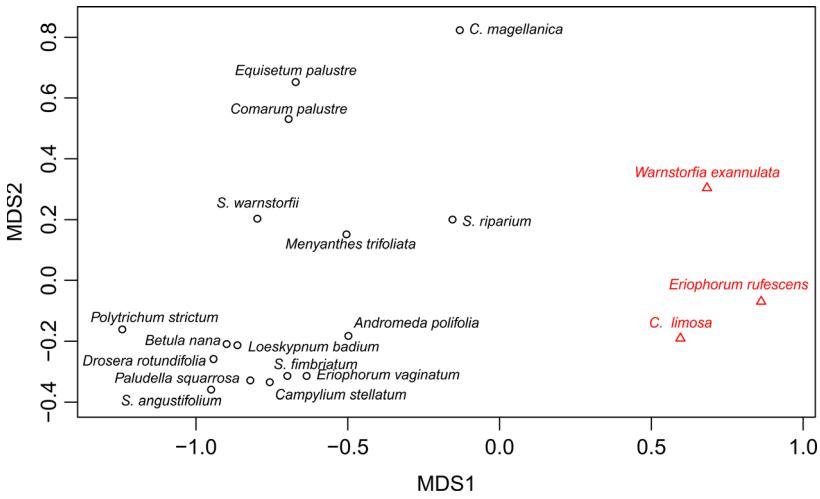

Figure 4. Non-metric multidimensional scaling (MDS) ordination axes and plant community clusters for Halssiaapa study site. The statistically significant (P-value < 0.05) indicator species for different clusters drawn on an ordination plot where non-metric multidimensional scaling axis 1 is on x-axis and axis 2 on y-axis. Cluster 1 is shown with black and cluster 2 with red. Species indicator values are given in Table S1. "C." refers to Carex and "S." to Sphagnum.

community clusters and also in PFTs, which mainly follow the wetness gradient at the fen so that shrubs and feather mosses are mostly found on string tops, while graminoids are most abundant in flarks. However, within-microform heterogeneity hampers the detectability of PFTs; for example, while graminoids are abundant in some flark patches, they are almost absent in others. The more coarse-scale variation, related to surface water impact of the stream, could also be seen in plant clusters and ordination axis (esp. MDS2 and Cluster 3, Fig. 2) and predicted well with remotely sensed data (Table 2).

Mapping performance was relatively poor, in general, in Lompolojänkkä. The modeling accuracy was the highest for *Salix*, MDS1, MDS2 and compositionally unique clusters 3 (*Salix* spp. adjacent to the stream) and 5 (oligotrophic fen edges) (Table 2). All of these mapped vegetation properties were more linked to coarse-scale vegetation patterns instead of fine-resolution spatial heterogeneity. This demonstrates that not all vegetation variability in the northern peatlands have a fine-scale character, in contrast to what has been discussed before (Lehmann et al. 2016; Mercer and Westbrook 2016; Lees et al. 2018; Palace et al. 2018). Furthermore, although there is also a finer-scale spatial heterogeneity in the Lompolojänkkä study site, visible, for example, in plant community clusters, it could not be captured with remote sensing regressions. The low detectability may be hampered by low topographical variation or overlapping clusters. The use of other remote sensing datasets, such as hyperspectral imagery (Middleton et al. 2012; Cole et al. 2013; Harris et al. 2015) or multispectral or thermal UAV data, could assist in mapping the PFTs and plant communities at a fine scale.

In Halssiaapa, the performance in PFT and plant community cluster regressions were between that of Kaamanen and Lompolojänkkä (Table 2). However, the optimal number of clusters was only two, an amount which does not realistically illustrate the heterogeneity in vegetation (Fig. 4). For instance, according to visual interpretation in the field, at least three distinct microforms can be found, namely, strings, lawns and flarks. This shows the elusive vegetation patterns in the fen. Although a string-lawn-flark pattern is visible in the fen, the transitional zones between different microforms are fuzzy and not as abrupt as in Kaamanen, which make the delineation and clustering of distinct plant communities difficult. Furthermore, there is also variability in the trophic status patterns within the fen, which could not be well captured with floristic or remote sensing methods. It has also been discussed that the trophic status is not visible even in soil properties within the fen (Mikola et al., unpublished data). These findings illustrate that even the remote sensing methods developed to detect continuous vegetation patterns (Rocchini 2014; Harris et al. 2015) may be insufficient in some cases to map vegetation. In these cases, a solution could be combining vegetation and remote sensing data in ordination or clustering approaches (Rapinel et al. 2018). In PFT regressions, the performance was especially good for *Sphagnum* and also relatively good for wet brown mosses, shrubs and forbs (Table 2). The study site has partly continuous *Sphagnum* and wet brown moss cover with few vascular plants on top, and the mosses have distinct spectral properties when compared to areas covered by vascular plants, open water or bare peat. It has also been found that the areas covered by *Sphagnum* have unique soil properties (Mikola et al., unpublished data), which emphasizes the need for conducting PFT or species-specific mappings in some situations (Ustin and Gamon 2010; Schmidtlein et al. 2012; Cole et al. 2013; Kattenborn et al. 2019).

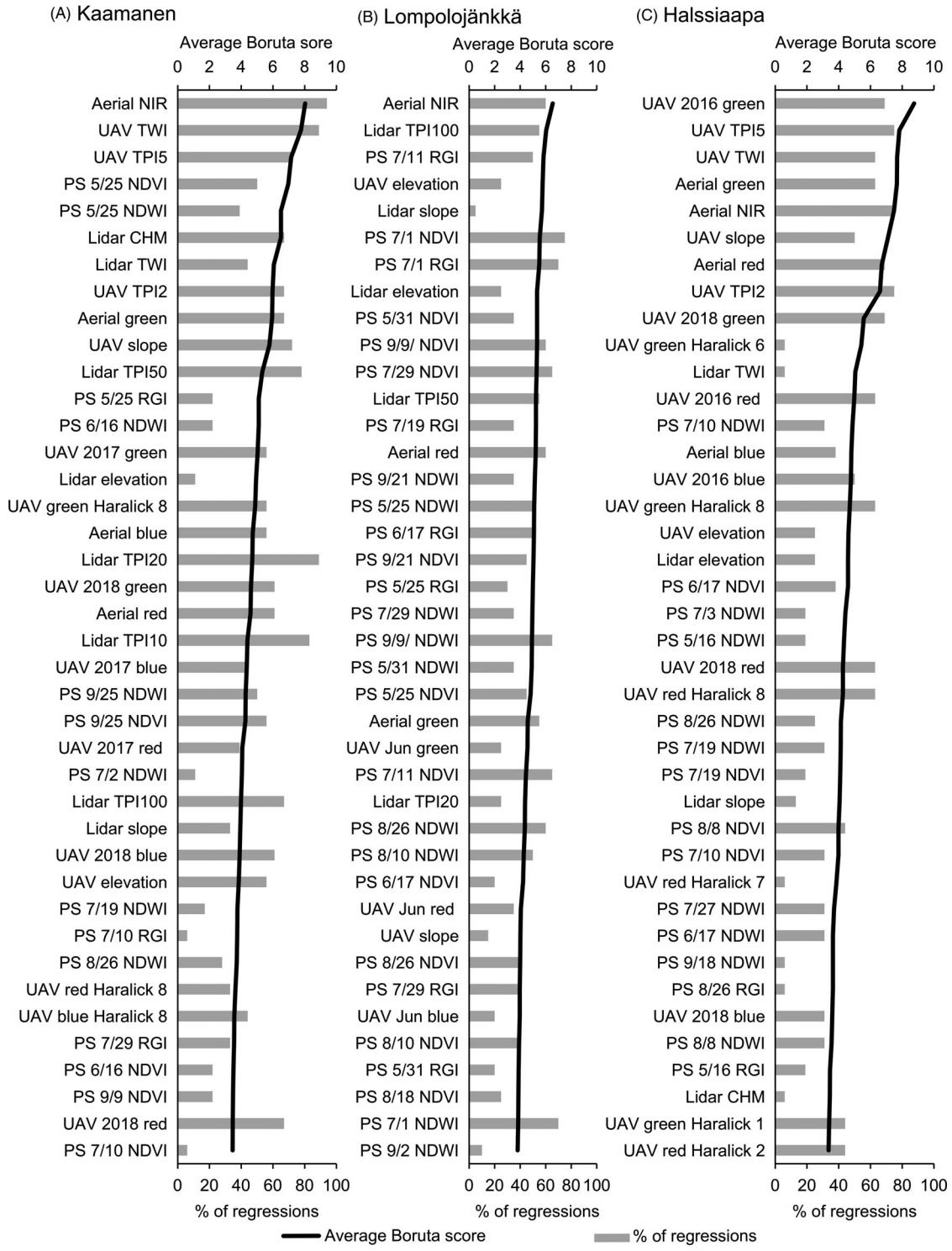

Figure 5. The 40 most important features for (A) Kaamanen, (B) Lompolojänkkä and (C) Halssiaapa based on average Boruta score over all regressions. Average Boruta score is shown with black line and the percentage of regressions in which the feature was deemed important with gray columns. Used abbreviations: CHM, canopy height model; NDVI, normalized difference vegetation index; NDWI, normalized difference water index; NIR, near infrared; PS, PlanetScope; RGI, red-green index; TPI, topographic position index; TWI, topographic wetness index; UAV, unmanned aerial vehicle. Haralick features are numbered as follows: 1, energy; 2, entropy; 3, correlation; 4, inverse difference moment; 5, inertia; 6, cluster shade; 7, cluster prominence; 8, Haralick correlation.

It can be argued that PFTs, ordination axes and fuzzy clusters complement each other and reveal different types of vegetation patterns. PFT maps are valuable in mapping ecosystem processes (Ustin and Gamon 2010; Schmidtlein et al. 2012; Kattenborn et al. 2019), but their drawbacks seem to be low mapping accuracies in some cases. If the %-cover of PFT in question is very low and its spectral properties are not very distinct from other PFTs, it can be expected that it is difficult or even impossible to map it using remotely sensed data. There have also been approaches for finding such PFT classifications and traits that can be mapped using remote sensing (Kattenborn et al. 2019), but such classifications should also be linked to ecosystem functioning of interest. However, as suggested before, there is a need for finding PFTs that are optimal in their separability from an ecological, environmental and remote sensing perspective (Harris et al. 2015; Kattenborn et al. 2019). PFT maps could also be combined with categorical vegetation maps. For example, PFT maps could show areas of high abundance of a specific PFT (e.g. shrubs, forbs) within a specific plant community or land cover. These composite maps would illustrate multiple aspects of vegetation simultaneously. When compared with ordination axes, plant community clusters have a more straightforward ecological interpretation and could thus be a recommended approach. However, the ability to distinguish ordination axes and plant communities with remotely sensed data varies between and within study sites, suggesting that multiple approaches could be used.

In most of the regressions, multiple different types of features were deemed important by Boruta, and these features were from multiple data sources (Fig. 5, Tables S2–S4). This suggests that the inclusion of different datasets is required for achieving the highest explanatory capacities when mapping vegetation patterns; the finding is also supported by previous research which has reported the benefits of versatile data in length (e.g. Chen et al. 2017; Räsänen and Virtanen 2019). Similar pattern of feature importance was visible both in spectral and structural features; typically coarser-resolution features were more important in Lompolojänkkä, whereas in the two other study sites, both fine-scale and coarse-scale features were among the most important ones (Fig. 5, Tables S2–S4). Furthermore, this feature importance pattern was visible in all different types of regressions (i.e. PFTs, ordination axes and plant community clusters). In spectral features, UAV data were highly important in Kaamanen and Halssiaapa, whereas aerial and PS data were important in all study sites. With regards to topography, in Kaamanen, both UAV and lidar topography features were among the most important ones in many of the regressions, whereas in Lompolojänkkä lidar topography features were more important; and in Halssiaapa, most important topography features were mostly derived from UAV data.

Our results showed that high-resolution spectral and topography features were important when detecting fine-scale heterogeneity in vegetation patterns, especially evident in Kaamanen and Halssiaapa (Fig. 5). This further highlights the need to use centimeter-resolution data in some mapping cases, in particular if there is fine-scale variation in vegetation, land cover and topography in the study site (Lehmann et al. 2016; Lovitt et al. 2017; Palace et al. 2018). However, the relative importance of the UAV data was lower in Lompolojänkkä, showing that the usage of such data is not always a solution when attempting to detect spatial heterogeneity in vegetation from above. Furthermore, in earlier research, it has been shown that when centimeter-resolution UAV data are replaced with 0.5-m resolution aerial image data, almost equivalent performance in land-cover mapping is achieved (Räsänen and Virtanen 2019).

Our results showed mixed evidence when assessing the importance of textural features (Fig. 5, Tables S2–S4). The importance of texture was more prominent in Halssiaapa and Lompolojänkkä than in Kaamanen. This might be related to the fact that in Kaamanen, the performance in different regressions was higher and most of the vegetation patterns were easily identifiable also without texture. An earlier study conducted in Kaamanen showed that texture helps mapping performance in situations where there are few other features in the model; however, when the model includes multiple features from multiple datasets, texture might not be useful (Räsänen and Virtanen 2019). Nevertheless, our work indicates that there is between-site variation in the importance of textural (and also other) features in mapping tasks.

PS images were useful in detecting coarse-scale patterns and areas with distinct phenology within peatlands. In Kaamanen, the early summer PS images in particular helped in mapping the second MDS axis and plant community clusters (Table S2). The second MDS axis was linked to surface water impact and the clusters also differed in relation to the axis (Fig. 2). In visual inspection of the early summer PS images, it could be seen that areas close to the stream had a distinct spectral property due to spring flooding (i.e. low NDVI and high NDWI), but this pattern was not evident in the images taken later during the growing season. This highlights the need to include datasets from different phenological or hydrological phases in mapping tasks (Chen et al. 2017; Halabisky et al. 2018) or to include datasets of the optimal phenological stage (Cole et al. 2014; Juutinen et al. 2017). This could be seen also in Lompolojänkkä, where the good performance of the PS indices was probably linked to the fact that, with the PS indices, the peatland edge and riparian area

vegetation could be distinguished from the other areas in the peatland. The riparian areas are wetter and peatland edge drier than the rest of the peatland especially in the beginning of growing season. Furthermore, in mapping these patterns, the extra spectral information in the form of spectral indices relying on near-infrared reflectance was probably helpful.

Conclusions

We compared different remote sensing datasets and approaches for detecting spatial patterns of vegetation properties across three northern boreal peatland study sites. Our results highlight that there rarely is a one-size-fits-all approach with which peatland vegetation could be grouped and mapped; instead, the optimal strategies depend on the structure of peatland in question. We showed that there was notable between-site variation in mapping performance, there were differences between sites as to which kind of regressions (i.e. PFTs, ordination axes, plant community clusters) had the highest explanatory capacities, and that in all study sites different types of features derived from multiple data sources were among the most important ones in regressions. Based on these findings, we propose some suggestions for future mapping tasks. First, multiple different mapping approaches should be tested and evaluated, and the optimal mapping approach should be chosen based on the study site and need. Second, multiple different remote sensing datasets should be included in the mapping, including datasets capturing both structural and spectral properties of vegetation. Third, as different mapping approaches complement each other, multiple different maps, including maps showing one vegetation characteristic and composite maps combining multiple characteristics, should be produced to illustrate the different aspects of vegetation within the studied landscape. Uncertainties, caveats and benefits should be explicitly reported for each map.

ACKNOWLEDGMENTS

We thank Valtteri Hyöky, Olivia Kuuri-Riutta and Tiia Määttä for field work assistance and Kari Mäenpää, Pasi Korpelainen and Anton Kuzmin for conducting the UAV flights. The work was supported by the Academy of Finland (grants 296423 [AR, SJ, TV], 308513 [AR, TV], 296888 and 314799 [MA] and 308511 [AL]) and Strategic Research Council, Academy of Finland grant 312559 [TK].

References

Anderson, M. J. 2001. A new method for non-parametric multivariate analysis of variance. *Austral Ecol.* **26**, 32–46.

Aurela, M., J. P. Tuovinen, and T. Laurila. 1998. Carbon dioxide exchange in a subarctic peatland ecosystem in northern Europe measured by the eddy covariance technique. *J. Geophys. Res. Atmos.* **103**, 11289–11301.

Aurela, M., T. Laurila, and J. P. Tuovinen. 2004. The timing of snow melt controls the annual CO_2 balance in a subarctic fen. *Geophys. Res. Lett.* **31**, 16111–16114.

Aurela, M., A. Lohila, J. P. Tuovinen, J. Hatakka, T. Riutta, and T. Laurila. 2009. Carbon dioxide exchange on a northern boreal fen. *Boreal Environ. Res.* **14**, 699–710.

Berner, L. T., P. Jantz, K. D. Tape, and S. J. Goetz. 2018. Tundra plant aboveground biomass and shrub dominance mapped across the North Slope of Alaska. *Environ. Res. Lett.* **13**, 035002.

Böhner, J., and T. Selige. 2006. Spatial prediction of soil attributes using terrain analysis and climate regionalisation. Pp. 13–28 in J. Böhner, K.R. McCloy, J. Strobl, eds. *SAGA – analysis and modelling applications. Göttinger Geographische Abhandlungen 115*. Goltze, Göttingen, Germany.

Bradley-Cook, J. I., and R. A. Virginia. 2018. Landscape variation in soil carbon stocks and respiration in an Arctic tundra ecosystem, west Greenland. *Arct. Antarct. Alp. Res.* **50**, S100024.

Bray, J. R., and J. T. Curtis. 1957. An ordination of the upland forest communities of Southern Wisconsin. *Ecol. Monogr.* **27**, 325–349.

Breiman, L. 2001. Random forests. *Mach. Learn* **45**, 5–32.

Campello, R. J. G. B., and E. R. Hruschka. 2006. A fuzzy extension of the silhouette width criterion for cluster analysis. *Fuzzy Sets Syst.* **157**, 2858–2875.

Chapin, F. S. III, M. S. Bret-Harte, S. E. Hobbie, and H. Zhong. 1996. Plant functional types as predictors of transient responses of arctic vegetation to global change. *J. Veg. Sci.* **7**, 347–358.

Chen, B., B. Huang, and B. Xu. 2017. Multi-source remotely sensed data fusion for improving land cover classification. *ISPRS J. Photogramm. Remote Sens.* **124**, 27–39.

Chen, W., X. Li, H. He, and L. Wang. 2018. Assessing different feature sets' effects on land cover classification in complex surface-mined landscapes by ZiYuan-3 satellite imagery. *Remote Sens.* **10**, 23.

Clark, M. L., T. M. Aide, H. R. Grau, and G. Riner. 2010. A scalable approach to mapping annual land cover at 250 m using MODIS time series data: a case study in the Dry Chaco ecoregion of South America. *Remote Sens. Environ.* **114**, 2816–2832.

Cole, B., J. McMorrow, and M. Evans. 2013. Empirical modelling of vegetation abundance from airborne hyperspectral data for upland peatland restoration monitoring. *Remote Sens.* **6**, 716–739.

Cole, B., J. McMorrow, and M. Evans. 2014. Spectral monitoring of moorland plant phenology to identify a temporal window for hyperspectral remote sensing of peatland. *ISPRS J. Photogramm. Remote Sens.* **90**, 49–58.

Coops, N. C., M. Johnson, M. A. Wulder, and J. C. White. 2006. Assessment of QuickBird high spatial resolution imagery to detect red attack damage due to mountain pine beetle infestation. *Remote Sens. Environ.* **103**, 67–80.

R Core Team. 2018. *R: a language and environment for statistical computing*. R Foundation for Statistical Computing, Vienna, Austria.

Dallmeyer, A., M. Claussen, and V. Brovkin. 2019. Harmonising plant functional type distributions for evaluating Earth system models. *Clim. Past* **15**, 335–366.

Davidson, S. J., M. J. Santos, V. L. Sloan, K. Reuss-Schmidt, G. K. Phoenix, W. C. Oechel, et al. 2017. Upscaling CH_4 fluxes using high-resolution imagery in Arctic Tundra ecosystems. *Remote Sens.***9**, 1227.

Dinsmore, K. J., J. Drewer, P. E. Levy, C. George, A. Lohila, M. Aurela, et al. 2017. Growing season CH_4 and N_2O fluxes from a subarctic landscape in northern Finland; From chamber to landscape scale. *Biogeosciences* **14**, 799–815.

Duckworth, J. C., M. Kent, and P. M. Ramsay. 2000. Plant functional types: an alternative to taxonomic plant community description in biogeography? *Prog. Phys. Geogr.* **24**, 515–542.

Dufrêne, M., and P. Legendre. 1997. Species assemblages and indicator species: the need for a flexible asymmetrical approach. *Ecol. Monogr.* **67**, 345–366.

Feilhauer, H., U. Faude, and S. Schmidtlein. 2011. Combining Isomap ordination and imaging spectroscopy to map continuous floristic gradients in a heterogeneous landscape. *Remote Sens. Environ.* **115**, 2513–2524.

Ferraro, M. B., and P. Giordani. 2015. A toolbox for fuzzy clustering using the R programming language. *Fuzzy Sets Syst.* **279**, 1–16.

Fraixedas, S., A. Lindén, K. Meller, Å. Lindström, O. Keišs, J. A. Kålås, et al. 2017. Substantial decline of Northern European peatland bird populations: consequences of drainage. *Biol. Cons.* **214**, 223–232.

Franklin, S. E., and O. S. Ahmed. 2017. Object-based wetland characterization using radarsat-2 quad-polarimetric SAR data, landsat-8 OLI imagery, and airborne lidar-derived geomorphometric variables. *Photogramm. Eng. Remote Sensing* **83**, 27–36.

Guisan, A., S. B. Weiss, and A. D. Weiss. 1999. GLM versus CCA spatial modeling of plant species distribution. *Plant Ecol.* **143**, 107–122.

Halabisky, M., C. Babcock, and L. M. Moskal. 2018. Harnessing the temporal dimension to improve object-based image analysis classification of wetlands. *Remote Sens.* **10**, 1467.

Hall-Beyer, M. 2017. Practical guidelines for choosing GLCM textures to use in landscape classification tasks over a range of moderate spatial scales. *Int. J. Remote Sens.* **38**, 1312–1338.

Haralick, R. M., I. Dinstein, and K. Shanmugam. 1973. Textural features for image classification. *IEEE Trans. Syst. Man. Cybern.* **SMC-3**, 610–621.

Harris, A., R. Charnock, and R. M. Lucas. 2015. Hyperspectral remote sensing of peatland floristic gradients. *Remote Sens. Environ.* **162**, 99–111.

Hartley, A. J., N. MacBean, G. Georgievski, and S. Bontemps. 2017. Uncertainty in plant functional type distributions and its impact on land surface models. *Remote Sens. Environ.* **203**, 71–89.

Hugelius, G., T. Virtanen, D. Kaverin, A. Pastukhov, F. Rivkin, S. Marchenko, et al. 2011. High-resolution mapping of ecosystem carbon storage and potential effects of permafrost thaw in periglacial terrain, European Russian Arctic. *J. Geophys. Res. Biogeosci.* **116**. https://doi.org/10.1029/2010JG001606

Juutinen, S., T. Virtanen, V. Kondratyev, T. Laurila, M. Linkosalmi, J. Mikola, et al. 2017. Spatial variation and seasonal dynamics of leaf-area index in the arctic tundra-implications for linking ground observations and satellite images. *Environ. Res. Lett.* **12**, 095002.

Kalacska, M., M. Lalonde, and T. R. Moore. 2015. Estimation of foliar chlorophyll and nitrogen content in an ombrotrophic bog from hyperspectral data: scaling from leaf to image. *Remote Sens. Environ.* **169**, 270–279.

Kattenborn, T., F. E. Fassnacht, and S. Schmidtlein. 2019. Differentiating plant functional types using reflectance: which traits make the difference? *Remote Sens. Ecol. Conserv.* **5**:5–19.

Krishnapuram, R., A. Joshi, O. Nasraoui, and L. Yi. 2001. Low-complexity fuzzy relational clustering algorithms for Web mining. *IEEE Trans. Fuzzy Syst.* **9**, 595–607.

Kruskal, J. B. 1964a. Multidimensional scaling by optimizing goodness of fit to a nonmetric hypothesis. *Psychometrika* **29**, 1–27.

Kruskal, J. B. 1964b. Nonmetric multidimensional scaling: a numerical method. *Psychometrika* **29**, 115–129.

Kursa, M. B., and W. R. Rudnicki. 2010. Feature selection with the boruta package. *J. Stat. Softw.* **36**, 1–13.

Laine, A. M., L. Mehtätalo, A. Tolvanen, S. Frolking, and E. S. Tuittila. 2019. Impacts of drainage, restoration and warming on boreal wetland greenhouse gas fluxes. *Sci. Total Environ.* **647**, 169–181.

Lees, K. J., T. Quaife, R. R. E. Artz, M. Khomik, and J. M. Clark. 2018. Potential for using remote sensing to estimate carbon fluxes across northern peatlands – a review. *Sci. Total Environ.* **615**, 857–874.

Lehmann, J. R. K., W. Münchberger, C. Knoth, C. Blodau, F. Nieberding, T. Prinz, et al. 2016. High-resolution classification of south patagonian peat bog microforms reveals potential gaps in up-scaled CH_4 fluxes by use of Unmanned Aerial System (UAS) and CIR imagery. *Remote Sens.* **8**, 173.

Liaw, A., and M. Wiener. 2002. Classification and regression by random forest. *R. News* **2**, 18–22.

Lohila, A., T. Penttila, S. Jortikka, T. Aalto, P. Anttila, E. Asmi, et al. 2015. Preface to the special issue on integrated research of atmosphere, ecosystems and environment at Pallas. *Boreal Environ. Res.* **20**, 431–454.

Loisel, J., S. van Bellen, L. Pelletier, J. Talbot, G. Hugelius, D. Karran, et al. 2017. Insights and issues with estimating northern peatland carbon stocks and fluxes since the Last Glacial Maximum. *Earth Sci. Rev.* **165**, 59–80.

Lovitt, J., M. M. Rahman, and G. J. McDermid. 2017. Assessing the value of UAV photogrammetry for characterizing terrain in complex peatlands. *Remote Sens.* **9**, 715.

Maanavilja, L., T. Riutta, M. Aurela, M. Pulkkinen, T. Laurila, and E. S. Tuittila. 2011. Spatial variation in CO_2 exchange at a northern aapa mire. *Biogeochemistry* **104**, 325–345.

McFeeters, S. K. 1996. The use of the Normalized Difference Water Index (NDWI) in the delineation of open water features. *Int. J. Remote Sens.* **17**, 1425–1432.

McPartland, M. Y., E. S. Kane, M. J. Falkowski, R. Kolka, M. R. Turetsky, B. Palik, et al. 2019. The response of boreal peatland community composition and NDVI to hydrologic change, warming, and elevated carbon dioxide. *Global Change Biol.* **25**, 93–107.

Mercer, J. J., and C. J. Westbrook. 2016. Ultrahigh-resolution mapping of peatland microform using ground-based structure from motion with multiview stereo. *J. Geophys. Res.-Biogeo.* **121**, 2901–2916.

Middleton, M., P. Närhi, H. Arkimaa, E. Hyvönen, V. Kuosmanen, P. Treitz, et al. 2012. Ordination and hyperspectral remote sensing approach to classify peatland biotopes along soil moisture and fertility gradients. *Remote Sens. Environ.* **124**, 596–609.

Mishra, V. N., R. Prasad, P. K. Rai, A. K. Vishwakarma, and A. Arora. 2018. Performance evaluation of textural features in improving land use/land cover classification accuracy of heterogeneous landscape using multi-sensor remote sensing data. *Earth Sci. Inf.* **12**, 71–86.

Oksanen, J., F. G. Blanchet, M. Friendly, R. Kindt, P. Legendre, D. McGlinn, et al. 2018. vegan: Community Ecology Package. R package version 2.5-1. In

Palace, M., C. Herrick, J. DelGreco, D. Finnell, A. J. Garnello, C. McCalley, et al. 2018. Determining subarctic peatland vegetation using an unmanned aerial system (UAS). *Remote Sens.* **10**, 1498

Peichl, M., O. Sonnentag, and M. B. J. E. Nilsson. 2015. Bringing color into the picture: using digital repeat photography to investigate phenology controls of the carbon dioxide exchange in a boreal mire. *Ecosystems* **18**, 115–131.

Poulter, B., N. MacBean, A. Hartley, I. Khlystova, O. Arino, R. Betts, et al. 2015. Plant functional type classification for earth system models: results from the European Space agency's land cover climate change initiative. *Geosci. Model Dev.* **8**, 2315–2328.

Prošek, J., and P. Šímová. 2019. UAV for mapping shrubland vegetation: does fusion of spectral and vertical information derived from a single sensor increase the classification accuracy? *Int. J. Appl. Earth Obs. Geoinf.* **75**, 151–162.

Rapinel, S., N. Rossignol, L. Hubert-Moy, J. B. Bouzillé, and A. Bonis. 2018. Mapping grassland plant communities using a fuzzy approach to address floristic and spectral uncertainty. *Appl. Veg. Sci.* **21**, 678–693.

Räsänen, A., and T. Virtanen. 2019. Data and resolution requirements in mapping vegetation in spatially heterogeneous landscapes. *Remote Sens. Environ.*. **4**, 20

Räsänen, A., S. Juutinen, M. Aurela, and T. Virtanen. 2019a. Predicting aboveground biomass in Arctic landscapes using very high spatial resolution satellite imagery and field sampling. *Int. J. Remote Sens.* **40**, 1175–1199.

Räsänen, A., S. Juutinen, E. S. Tuittila, M. Aurela, and T. Virtanen. 2019b. Comparing ultra-high spatial resolution remote sensing methods in mapping peatland vegetation. *J. Veg. Sci.*, **30**:1016–1026.

Rautiainen, M., P. Lukeš, L. Homolová, A. Hovi, J. Pisek, and M. Mõttus. 2018. Spectral properties of coniferous forests: a review of in situ and laboratory measurements. *Remote Sens.* **10**, 207.

Riihimäki, H., M. Luoto, and J. Heiskanen. 2019. Estimating fractional cover of tundra vegetation at multiple scales using unmanned aerial systems and optical satellite data. *Remote Sens. Environ.* **224**, 119–132.

Rocchini, D. 2014. Fuzzy species distribution models: a way to represent plant communities spatially. *J. Veg. Sci.* **25**, 317–318.

Rouse, J. W. J., R. H. Haas, J. A. Schell, and D. W. Deering. 1974. Monitoring vegetation systems in the Great Plains with ERTS. Pp. 309–317 *in* S. C. Freden, E. P. Mercanti and M. A. Becker, eds.*Third earth resources technology satellite-1 symposium*. NASA, Washington, DC.

Saarimaa, M., K. Aapala, S. Tuominen, J. Karhu, M. Parkkari, and A. J. B. Tolvanen. 2019. Predicting hotspots for threatened plant species in boreal peatlands. *Biodivers. Conserv.* **28**:1173–1204.

Sankey, T. T., J. McVay, T. L. Swetnam, M. P. McClaran, P. Heilman, and M. Nichols. 2018. UAV hyperspectral and lidar data and their fusion for arid and semi-arid land vegetation monitoring. *Remote Sens. Ecol. Conserv.* **4**, 20–33.

Schmidtlein, S., H. Feilhauer, and H. Bruelheide. 2012. Mapping plant strategy types using remote sensing. *J. Veg. Sci.* **23**, 395–405.

Schneider, J., L. Kutzbach, and M. J. B. Wilmking. 2012. Carbon dioxide exchange fluxes of a boreal peatland over a complete growing season, Komi Republic, NW Russia. *Biogeochemistry* **111**, 485–513.

Scholefield, P., D. Morton, G. McShane, L. Carrasco, M. G. Whitfield, C. Rowland, et al. 2019. Estimating habitat extent and carbon loss from an eroded northern blanket bog using UAV derived imagery and topography. *Prog. Phys. Geogr.: Earth Environ.* **43**, 282–298.

Shadaydeh, M., A. Zlinszky, A. Manno-Kovacs, and T. Sziranyi. 2017. Wetland mapping by fusion of airborne laser

scanning and multi-temporal multispectral satellite imagery. *Int. J. Remote Sens.* **38**, 7422–7440.

Planet Team. 2017. *Planet application program interface: in space for life on earth*. Planet, San Francisco, CA.

Ustin, S. L., and J. A. Gamon. 2010. Remote sensing of plant functional types. *New Phytol.* **186**, 795–816.

Waddington, J. M., P. J. Morris, N. Kettridge, G. Granath, D. K. Thompson, and P. A. Moore. 2015. Hydrological feedbacks in northern peatlands. *Ecohydrology* **8**, 113–127.

Supporting Information

Additional supporting information may be found online in the Supporting Information section at the end of the article.

Figure S1. Ordination dimensions and plant community clusters for Kaamanen study site.

Figure S2. Ordination axes and plant community clusters for Lompolojänkkä study site.

Figure S3. Ordination axes and plant community clusters for Halssiaapa study site.

Table S1. Clusters, their statistically significant indicator species (P-value < 0.05) and corresponding indicator values for each study area.

Table S2. Boruta scores for non-rejected features in each regression in Kaamanen study site.

Table S3. Boruta scores for non-rejected features in each regression in Lompolojänkkä study site.

Table S4. Boruta scores for non-rejected features in each regression in Halssiaapa study site.

